AJNR

3DFT MR angiography of carotid and basilar arteries.

W A Wagle, C L Dumoulin, S P Souza and H E Cline

3DFT MR Angiography of Carotid and Basilar Arteries

William A. Wagle[1]
Charles L. Dumoulin[2]
Steven P. Souza[2,3]
Harvey E. Cline[2]

Three-dimensional Fourier transform (3DFT) time-of-flight and two-dimensional Fourier transform (2DFT) projection phase-contrast MR angiography was performed in eight healthy volunteers and in 14 patients with known carotid artery or basilar artery occlusion, stenosis, or dissection. Comparative angiography was available in 13 cases (although in some cases the studies were separated by a number of months) and duplex sonography in one case. After localization of the carotid artery bifurcations by using 2DFT projection phase-contrast angiography, multiple 1.25-mm contiguous images were obtained with the 3DFT technique. In all cases, the lesions were identified on MR angiography. Because flow is detected in a manner that is independent of flow-induced phase shifts in the 3DFT time-of-flight technique, signal loss arising from complex flow and turbulence is minimized, yet the flow image remains sensitive to all velocity components of flow.

Applications of this technique are ideal for relatively straight vessels where flow is laminar, but it can also be used to evaluate the carotid artery bifurcations where flow becomes complex.

MR angiography is a product of flow imaging techniques that have been developed over the past several years [1–7]. The two most common techniques are time-of-flight and motion-induced phase-shift flow imaging. In time-of-flight angiography, a bolus of blood is "tagged" in one region and is allowed to move into another region before sampling is obtained. A tagging mechanism such as inversion, saturation, or relaxation is chosen to differentiate moving blood from surrounding stationary tissue. With this technique, the detectable range of spin movement is limited by the velocity of the blood and by the T1 of the blood, which restricts the lifetime of the tagging [1]. In the second method, flow information is obtained from motion-induced phase shifts in transverse spin magnetization [7]. Because stationary tissue has no flow-induced phase shift, it can be differentiated from signals arising from flowing blood, which will generate a phase shift proportional to its velocity when that velocity is coincident with the direction of the applied gradient. This technique is not limited by the lifetime of the tagged bolus and can measure relatively slow flow, but its major disadvantage is loss of signal because of dephasing in areas of complex or turbulent flow. This poses a formidable problem in the evaluation of the carotid artery bifurcation where complex flow arises even in normal arteries. Dephasing gives rise to loss of signal, which in turn generates a false-positive "stenosis." Our experience with cardiac-gated and cine phase-contrast angiography, which has been reported [8], yielded an improvement on this technique but still did not completely resolve the problem of the false-positive stenosis caused by dephasing artifacts.

In late 1987, three-dimensional Fourier transform (3DFT) was added to the existing technology of gradient-recalled acquisition in the steady state (GRASS) angiography, and our subsequent experience with this technique forms the basis of this report.

[1] Departments of Radiology and Neurology, Albany Medical Center, Albany, NY 12208. Address reprint requests to W. A. Wagle.

[2] General Electric Corporate Research & Development Center, Schenectady, NY 12301.

[3] General Electric Consulting Services, Albany, NY 12205.

Materials and Methods

All of the patients in this study had experienced either transient ischemic attacks, amaurosis fugax, or strokes that led to neurologic evaluation and subsequent cerebral angiography (13 cases) or duplex sonography (one case). All patients had either CT or MR before they had MR angiography, and in all cases MR angiography was performed as a follow-up to evaluate known lesions within the cervical carotid artery (12 cases) or basilar artery (two cases). In all cases MR angiography was performed after standard angiography, typically within a few months. Four of the 14 studies were postoperative follow-up studies for which only preoperative angiograms were available for comparison; all of these cases involved carotid artery stenosis or occlusion. One study in a case of severe basilar artery stenosis was performed at the Albany Medical Center on a 1.5-T Signa unit; all other studies were performed at the General Electric Corporate Research and Development Center in Schenectady, NY, on the 1.5-T Signa unit. The patients signed informed consents meeting the guidelines established by the Committee on Research Involving Human Subjects at the Albany Medical Center. All studies were monitored by a physician.

Patients were screened in the same manner as for routine MR imaging and special precautions were not necessary. A research surface coil was used in studies involving the cervical carotid artery and a routine head coil was used to study the intracranial arteries. Typically, a phase-contrast-projection angiogram was obtained to evaluate flow and to localize the carotid artery bifurcations. After this, two 3DFT time-of-flight angiograms, each containing 128 contiguous 1.25-mm images, were obtained in two 10-min series. The first series was performed without a saturation pulse and the second series with a saturation pulse that produced signal dropout within the normal arterial lumen. Subtraction of the data from these two series highlights arteries and further suppresses background signal. If the patient moved between the two data sets, there was imperfect subtraction, and the subtraction set was then less clear than either of the two original sets.

All studies were done under the research mode. In this mode, the pulse sequence is a GRASS technique, TR and TE are in the range of 38 and 14 msec, respectively, the field-of-view (FOV) is 16 cm, and the matrix is 256 × 128 × 128 (frequency × phase × phase). Frequency is in the anterior to posterior direction. The gradient specifications on the 1.5-T General Electric unit are maximally 1 G/cm, but typically only 0.5 G/cm is used in the flow-encoding direction for the phase-contrast technique. The gradient coils are shielded to suppress eddy currents. This provides improved suppression of background noise. The excitation slab is an 8-cm axial slab, which was chosen after determining the location of the carotid artery bifurcations on the two-dimensional Fourier transform (2DFT) phase-contrast study. The body coil is used for excitation and the surface coil is a receive coil only. A flow- or motion-compensation gradient is used in the time-of-flight 3DFT technique.

Data processing from the 3DFT study is done immediately after scanning and takes about 30 min. This can be performed in clinical sites; however, raw data must first be converted to image data before another study can begin. The postprocessing of image sets is performed with a utility program named BINOP, which is an acronym for binary operation. It allows subtraction or addition of image sets and provides postprocessing after image acquisition, minimizing the scanning time for the patient. Another postprocessing utility, IRMA, an acronym for image reformation using multiple algorithms, allows the projection of data taken in the axial plane to be projected in the coronal or sagittal plane or vice versa. This can be performed with the 3DFT technique because information is acquired within a volume and not in a slice.

We have found it beneficial to review the images on a CRT using the cine mode in addition to studying standard film images. This is helpful in following the carotid artery when the images are in the axial plane, especially at the common carotid artery bifurcation.

Results

Brief medical histories, standard angiographic results, and MR angiographic results are summarized in Table 1. There were two cases of basilar artery disease, one carotid artery dissecting aneurysm, two cases of unoperated carotid artery stenosis, and surprisingly, five cases of carotid artery dissection. Of the five cases of dissection, two were traumatic and three were spontaneous. Four of the studies were in patients who had undergone endarterectomies.

In the cases of nonocclusive carotid artery dissection (Figs. 1–3), the residual lumen maintained its normal signal, that is, on the nonsaturation series the lumen appeared hyperintense and on the saturation series it appeared hypointense. Luminal narrowing was seen clearly, and the dissection itself was quite apparent because of the ease of visualizing both the lumen and the wall of the artery in the axial plane. In the cases of carotid artery dissection with total occlusion (Fig. 4), the residual lumen no longer contained flowing blood, and on phase-contrast angiography there was total absence of signal within the region of the vessel. The same vessel was visualized on 3DFT, but its luminal signal resembled the surrounding stationary soft tissues of the neck and its actual diameter decreased, both because of the lack of flow. The decreased diameter of the carotid artery can be seen on routine angiography in cases of high-grade stenosis when contrast material opacifies the lumen of the artery above the stenosis, and it is presumed to be smaller in diameter above a total occlusion. Connectivity algorithms have also been developed that provide graphically beautiful images of the carotid arteries (Fig. 1F) that resemble "dye-cast" images [9]. This technique has been disappointing in clinical applications because it is not sensitive enough to visualize arteries with slow flow.

In our experience, localized plaque cannot be accurately visualized on phase-contrast-projection angiography because spatial resolution is limited by inherent artifacts due to dephasing (Fig. 5A). The time-of-flight 3DFT technique without saturation also suffers slightly from turbulence artifacts but much less so than with the phase-contrast-projection technique. Time-of-flight 3DFT with saturation appears to be the most effective technique for visualization of atheromatous plaque, which appears hyperintense relative to the hypointense lumen (Fig. 5C). The subtraction set of the two original data sets (saturation and nonsaturation) generates images with greater contrast (Fig. 5D). This BINOP program for the subtraction of data sets will work only if the patient can hold still for two consecutive 10-min sets. Even if the patient holds still for each of the sets but moves between sets, the subtraction set will have a misregistration artifact.

Artifacts are common in a number of the first and last images from the 128 total images obtained in the 3DFT imaging volume. We select an FOV of 16 cm, but the very

TABLE 1: Summary of Patients and Imaging Results

Case No.	Age	Gender	History	Angiography/ Sonography	MR Angiography/Interval Between Studies
1	55	F	R hemisphere TIA; bilateral endarterectomy	Severe bilateral stenosis	Postop: both ICAs open/3 mo
2	52	F	R hand weak; L ICA end-arterectomy	R CCA occlusion; 80% L ICA stenosis	Postop: improvement in L ICA to 40%/3 yr
3	36	M	L parietal infarction, spontaneous	Bilateral ICA dissections; L ICA reduced to "thread"	Bilateral ICA dissections; L ICA, improved flow/1 mo
4	63	M	Amaurosis fugax, OD, twice	40% stenosis, R ICA, on sonography; refused angiography	R ICA, 50% stenosis; L ICA normal/1 mo
5	44	M	Transient visual disturbance, OS; whistling noise, L skull base	Dissecting aneurysm, L cervical ICA	L ICA, dissecting aneurysm/4 mo
6	31	M	Aphasia and R hemiplegia after neck trauma	Acute occlusion of L ICA; R ICA, smooth occlusion (old)	No flow in either ICA/1 mo
7	73	M	Amaurosis fugax, OD	Severe bilateral ICA stenosis	Postop: both ICAs normal/16 mo
8	40	M	R parietal infarct several days after neck trauma	Total occlusion of R ICA due to dissection	Dissection well seen; no flow in R ICA/5 mo
9	68	F	Amaurosis fugax, OD	Total occlusion, L ICA; 75% stenosis R ICA	No flow in L ICA; flow present in R ICA; unable to do 3DFT/1 wk
10	54	M	Spontaneous headache, aphasia, R hemiparesis; improvement with Coumadin	Total occlusion of L ICA due to dissection	Return of flow in L ICA seen on both phase-contrast & 3DFT angiography/2 mo
11	59	M	Brainstem TIAs	Severely reduced flow in basilar, vertebral arteries	Reduced flow in vertebral arteries; phase-contrast study only/1 wk
12	72	M	Amaurosis fugax, OS; TIA, L hemisphere; bilateral endarterectomy	Severe bilateral ICA stenosis	Good flow in both ICAs/6 mo
13	58	M	Brainstem TIAs; Coumadin prescribed	Lower basilar stenosis	Basilar stenosis on 3DFT/7 mo
14	59	M	TIAs followed by L parietal infarct	Dissection of L ICA; stenosis without occlusion	Dissection of L ICA; flow present/1 mo

Note.—R = right; L = left; TIA = transient ischemic attack; Postop = postoperatively; ICA = internal carotid artery; CCA = common carotid artery; mo = month(s); yr = year(s); wk = week(s); OD = right eye; OS = left eye; 3DFT = three-dimensional Fourier transform.

best images are available over a distance of about 6 cm. This is because the time-of-flight technique is inherently limited by the T1 of flowing blood and by the velocity of that blood. In older patients with slower flow, the length of the imaging axis can fall slightly below 6 cm, and occasionally in younger patients with very good flow, the length goes beyond 6 cm.

If the FOV is 16 cm, or 160 mm, and there are 128 contiguous images, then the thickness of each image is 1.25 mm. This provides excellent spatial resolution in the axial plane of each image, but the greatest limitation is the distance that this technique can cover. Images can be obtained beyond 6 cm but the quality becomes degraded.

In the single case of a dissecting aneurysm of the carotid artery, the lesion was well seen on the 3DFT time-of-flight study, and in fact, the wall of the true lumen was better seen on this study than on the standard angiogram (Fig. 6A). This is because the aneurysm and true lumen overlap on all views on routine angiography, but on MR angiography the high

contrast resolution between flowing and nonflowing material is well differentiated so the wall of the true lumen adjacent to the aneurysm is clearly seen (Fig. 6C).

In the case of basilar artery stenosis (Fig. 7), the area of stenosis is seen with the 3DFT time-of-flight technique, and further manipulation of the data allows for a reconstruction so that all the axial images are reprojected into the lateral view (Fig. 7D). This is accomplished by the newly developed utility called IRMA. Although the site of stenosis is seen, the degree and length of stenosis is overestimated. The other case of basilar artery disease (case 11) involved a patient with severely reduced flow due to bilateral vertebral artery stenosis. This was the only study done at our institution, where shielded gradient coils have not yet been installed, and as such, the 3DFT studies were not optimal. In this case, the 2DFT phase-contrast technique was sensitive enough to detect the slow flow within both vertebral arteries, a finding that was demonstrated on standard angiography.
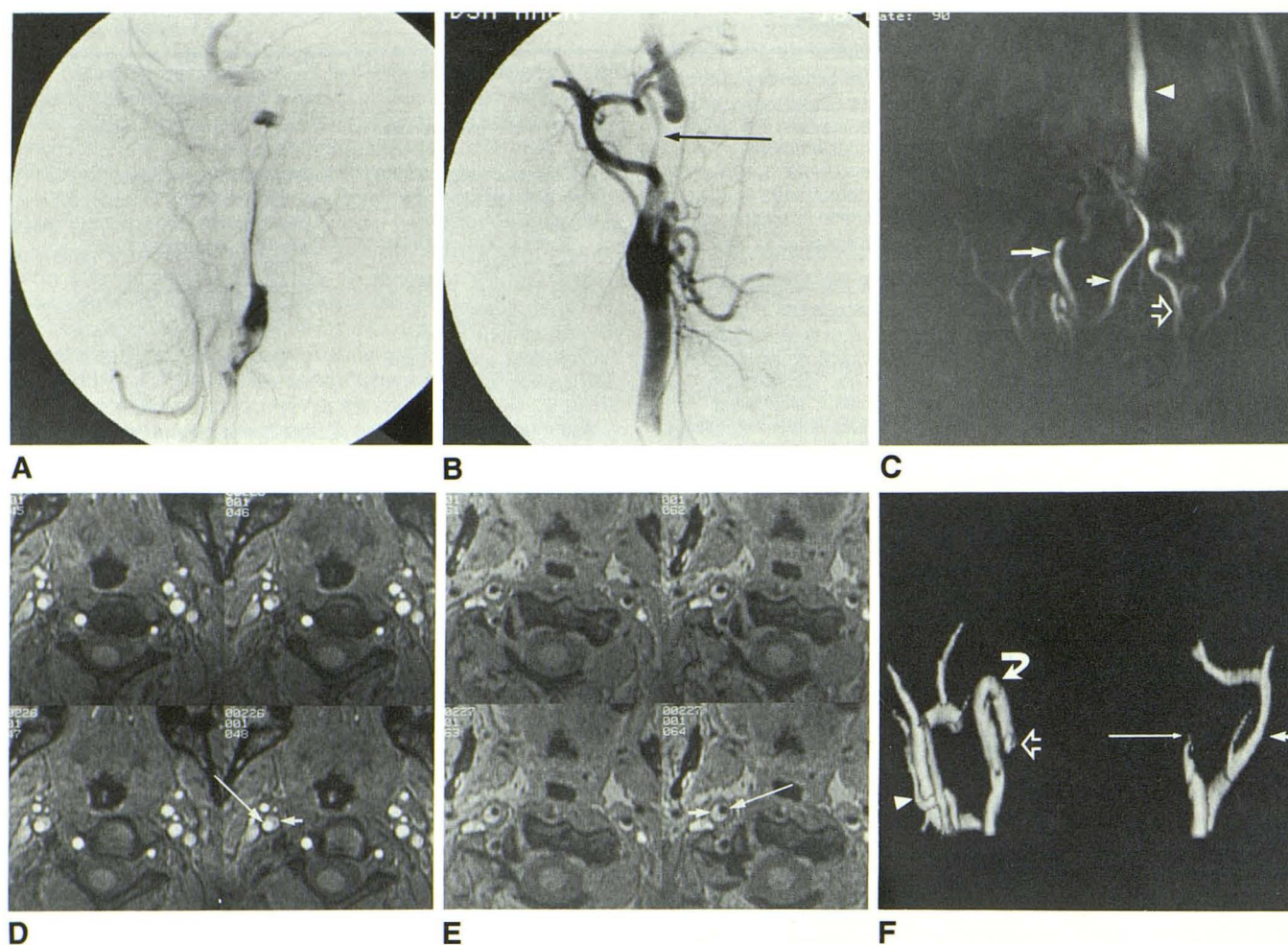
Fig. 1.—Case 3.

A, Left cervical internal carotid artery dissection, lateral view.

B, Right cervical internal carotid artery dissection (arrow), anteroposterior view.

C, Phase-contrast-projection angiogram shows right internal carotid artery (large solid arrow), left internal carotid artery (open arrow), right vertebral artery (small solid arrow), and superior sagittal sinus (arrowhead).

D, 3DFT time-of-flight axial images, sequentially numbered 45–48, each 1.25 mm, nonsaturation technique. Narrowed true lumen is normally hyperintense (long arrow) and helical dissection is less intense (short arrow).

E, 3DFT time-of-flight saturation technique. Narrowed internal carotid artery lumen is normally hypointense (long arrow), but dissection is abnormally hyperintense (short arrow). Note that dissection is to the right in D but to the left in E; this is because the dissection twists in a helical fashion and the two sets of images are not identical. The helical geometry is more obvious when viewed in cine mode.

F, 3D reconstruction using connectivity algorithm shows "dye-case" images of both carotid arteries. Right internal carotid artery has a prominent loop (curved arrow) and it appears to be totally occluded (open arrow). Right external carotid artery and its branches (arrowhead). Left internal carotid artery appears totally occluded (long straight solid arrow). Left external carotid artery with its branches (short straight solid arrow). Image is obtained by postprocessing information obtained with 3DFT technique, but it is not sensitive enough in detecting reduced flow because it shows both internal carotid branches to be occluded, when in fact they are narrowed but still patent.

Discussion

The flow-imaging techniques with which we have the most experience include 2DFT projection phase-contrast and 3DFT time-of-flight angiography. In 2DFT imaging, the three gradients are slice-select, frequency-encoding or "read," and phase-encoding. Phase change in flowing blood may occur along the direction of any of these gradients. This effect of motion is called spin dephasing or loss-of-phase coherence [1, 5]. These phase shifts can be prevented with the use of compensation gradient pulses. Because the slice-effect and readout gradient waveforms are bipolar, velocity-induced phase shifts arising from either can be compensated for by applying a bipolar gradient. The phase-encoding gradient pulses have a unipolar waveshape, and an appropriate compensated wave pulse contains a unipolar phase-encoding gradient and a bipolar flow-encoding pulse. Flow compensation of phase-encoding pulses is particularly important in the 3DFT technique because there are two orthogonal phase-encoding dimensions. Another artifact decreased by the use of this compensation gradient is the loss of signal intensity, which occurs when there are several velocity components within the region of interest, such as in the carotid artery bifurcation.
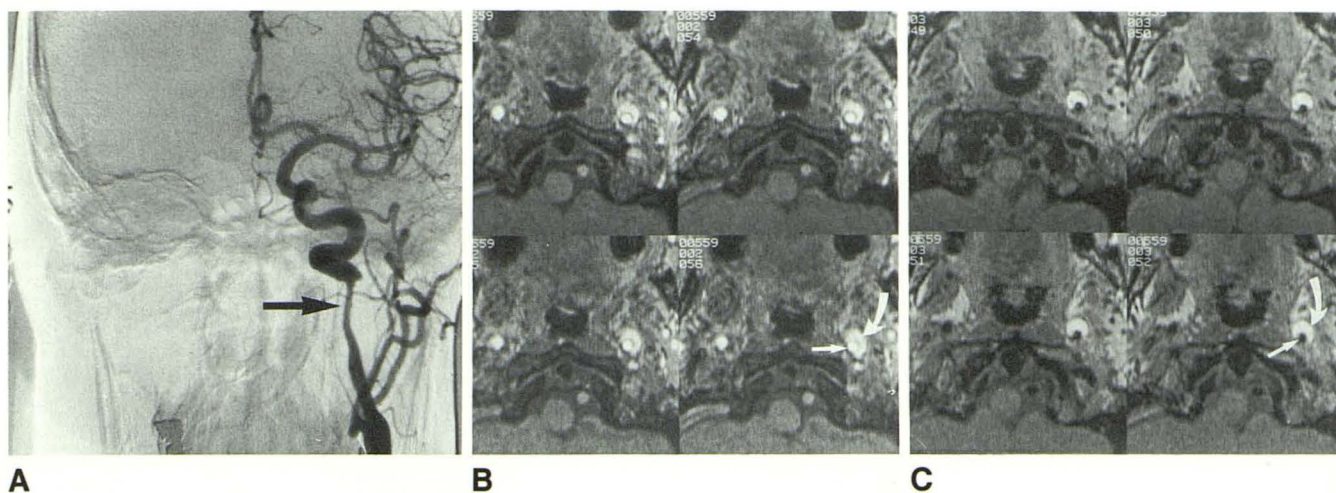
A

B

C

Fig. 2.—Case 14.
A, Left internal carotid dissection (*arrow*).
B, 3DFT nonsaturation image shows narrowed residual lumen (*straight arrow*) and helical dissection (*curved arrow*).
C, 3DFT saturation image. Narrowed lumen (*straight arrow*) is hypointense and dissection is hyperintense (*curved arrow*).
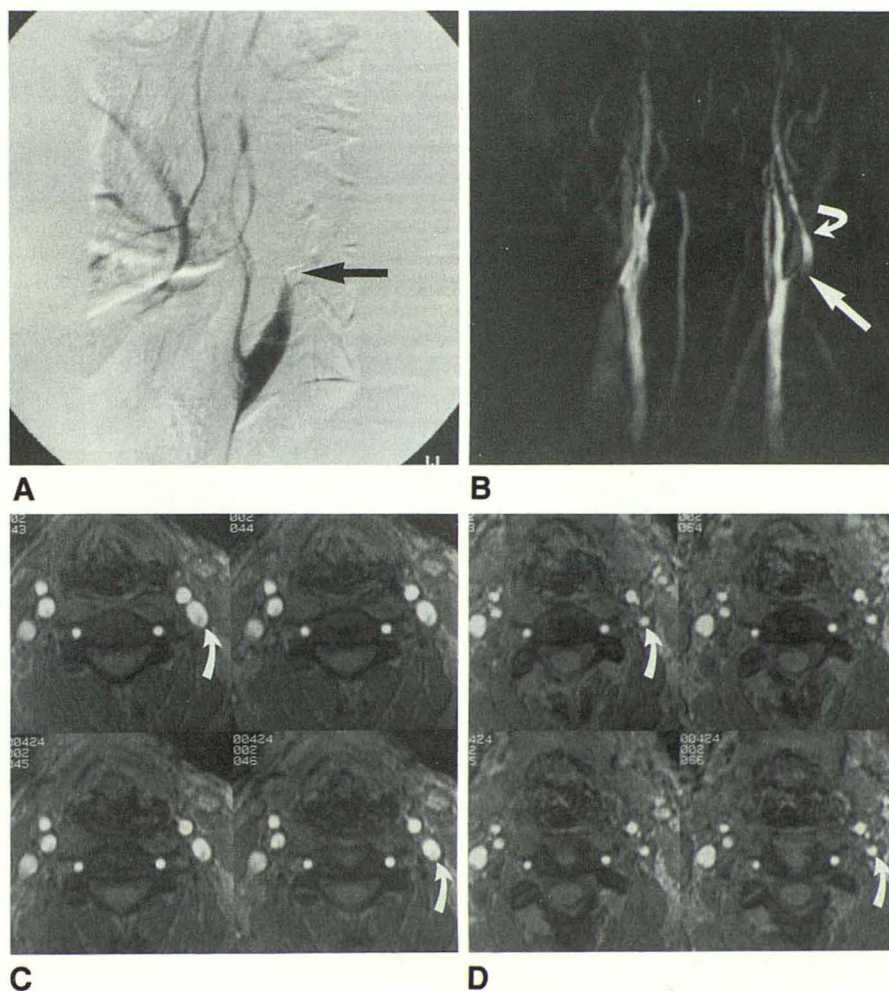

A

B

Fig. 3.—Case 10.
A, Dissection of left internal carotid artery with occlusion (*arrow*).
B, 2 months later. Phase-contrast study shows area of decreased signal at site of prior occlusion (*straight arrow*), but cephalad there is signal within internal carotid artery indicating return of flow (*curved arrow*).
C, 3DFT nonsaturation image shows normal proximal left internal carotid artery (*arrows*).
D, Axial images cephalad to C show normal signal but decreased diameter within left internal carotid artery (*arrows*).
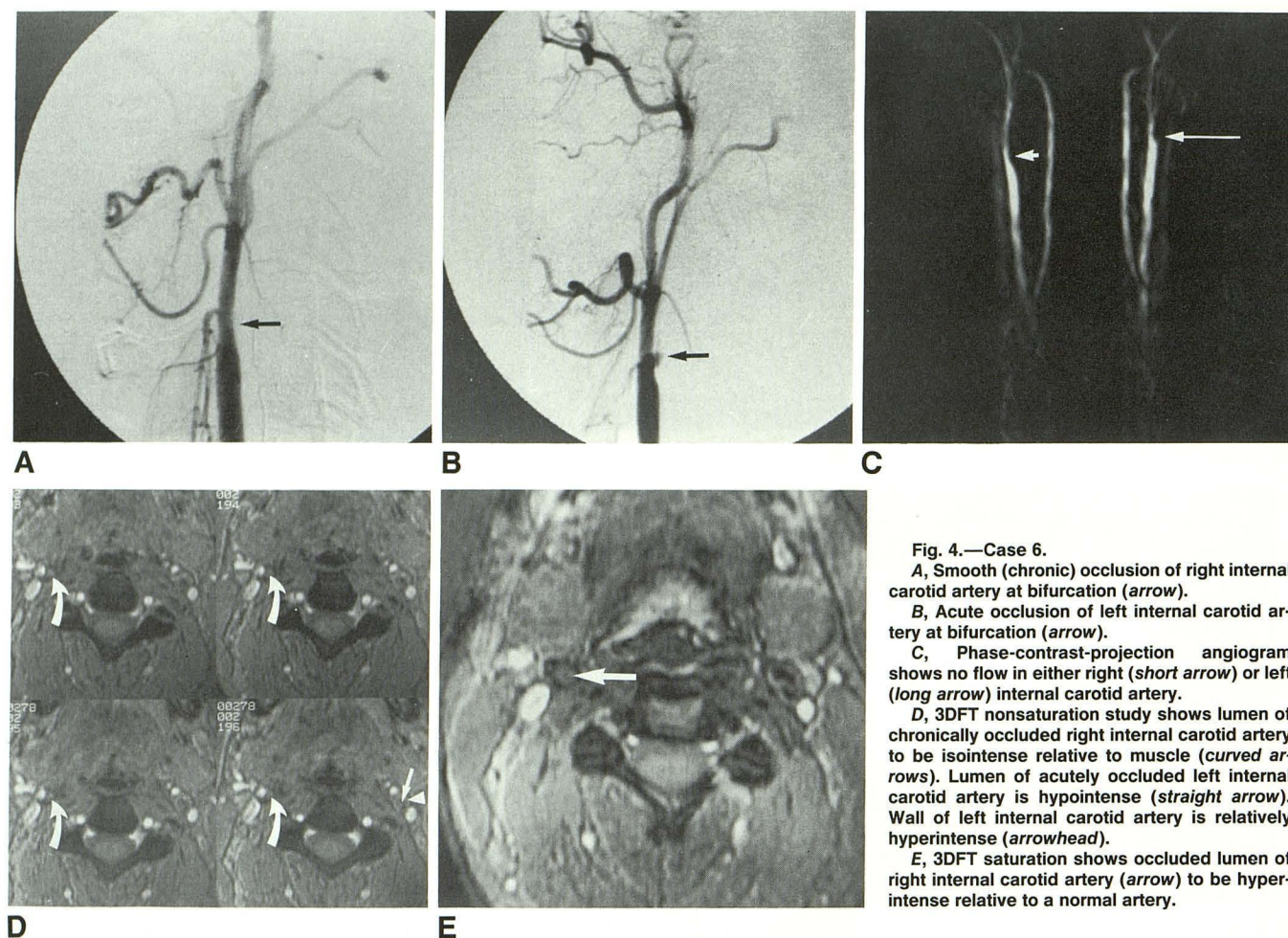
C

D

A

B

C

D

E

Fig. 4.—Case 6.

A, Smooth (chronic) occlusion of right internal carotid artery at bifurcation (*arrow*).

B, Acute occlusion of left internal carotid artery at bifurcation (*arrow*).

C, Phase-contrast-projection angiogram shows no flow in either right (*short arrow*) or left (*long arrow*) internal carotid artery.

D, 3DFT nonsaturation study shows lumen of chronically occluded right internal carotid artery to be isointense relative to muscle (*curved arrows*). Lumen of acutely occluded left internal carotid artery is hypointense (*straight arrow*). Wall of left internal carotid artery is relatively hyperintense (*arrowhead*).

E, 3DFT saturation shows occluded lumen of right internal carotid artery (*arrow*) to be hyperintense relative to a normal artery.

In the 3DFT technique, the data are collected simultaneously from the entire imaging volume by exciting a slab of tissue encompassing the volume of interest, which is smaller than the FOV. To "obtain slices" from this volume, a variable phase-encoding gradient is applied. Thus, to obtain 128 contiguous 1.25-mm images within the 16-cm FOV, 128 phase-encoding steps are necessary. In 2DFT, as many slices as there is time available are excited during one TR cycle. To obtain 10 slices in 2DFT, the total imaging time increases tenfold relative to a scan of equal TR. There are several advantages to 3DFT imaging. It allows acquisition of very thin contiguous slices with minimal interslice crosstalk and provides higher signal-to-noise because the signal-to-noise ratio increases as the square root of the number of phase encodings perpendicular to the imaging plane [10].

Flow information can be obtained from the x, y, or z components of flow, that is, any of the three orthogonal vectors of space. In order to combine the flow data from these three vectors, three different data sets are acquired and the postprocessing algorithm BINOP is applied. This is more pertinent to imaging of the cerebral vasculature where the arteries bend in several areas, whereas the cervical carotid arteries are relatively straight. For the cervical carotid artery studies using 3DFT time-of-flight, we acquire flow information in all three axes simultaneously. BINOP can still be applied to subtract data sets, as was explained in Materials and Methods. IRMA is applied to reproject axial images into the sagittal or coronal plane (Fig. 7D). Currently we are performing cerebral vascular studies with phase-contrast 3DFT and obtaining three different data sets, which are combined to give a single set of 128 images that contains flow information from the three vectors in space; this work will be the basis of a future report.

BINOP is applicable to both 2DFT phase-contrast and to 3DFT time-of-flight techniques because it is a postprocessing function rather than a pulse-sequence technique. Such postprocessing cannot improve on the information content of the original images, but by combining pairs of images, more of that information can be presented at once. The carotid arteries are relatively straight vessels that align with the long axis of the patient and, by convention in MR, lie within the z direction of flow. The z direction provides the greatest signal or flow information, but the best images can be obtained by taking the modulus (square root of the sum of the squares) of all

Fig. 5.—Case 4.

A, Left carotid bifurcation appears normal (*arrow*) and right carotid bifurcation appears "stenotic" (*arrowhead*) on phase projection angiogram.

B, 3DFT time-of-flight nonsaturation image shows 50% stenosis due to posteromedial plaque, which has low signal intensity (*straight arrow*); normal lumen maintains a high signal intensity (*curved arrow*).

C, 3DFT time-of-flight saturation shows same plaque as in *B*, but now lesion has high signal intensity (*straight arrow*) and residual lumen has decreased intensity (*curved arrow*).

D, Subtraction of saturation and nonsaturation data provides images that highlight arteries. Plaque has decreased signal (*short arrow*) and residual lumen has increased signal (*long arrow*).
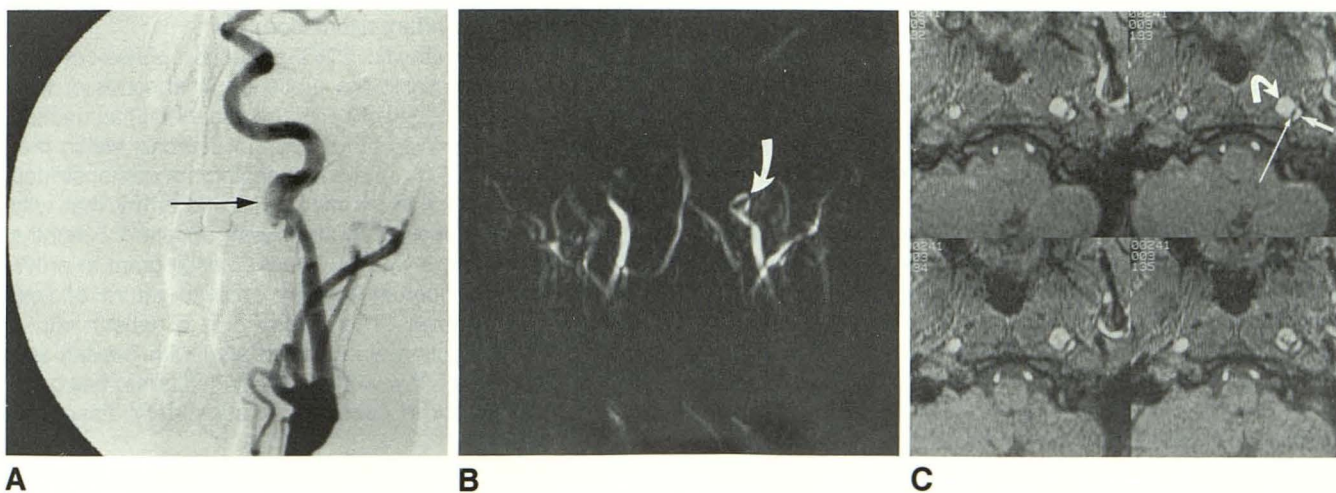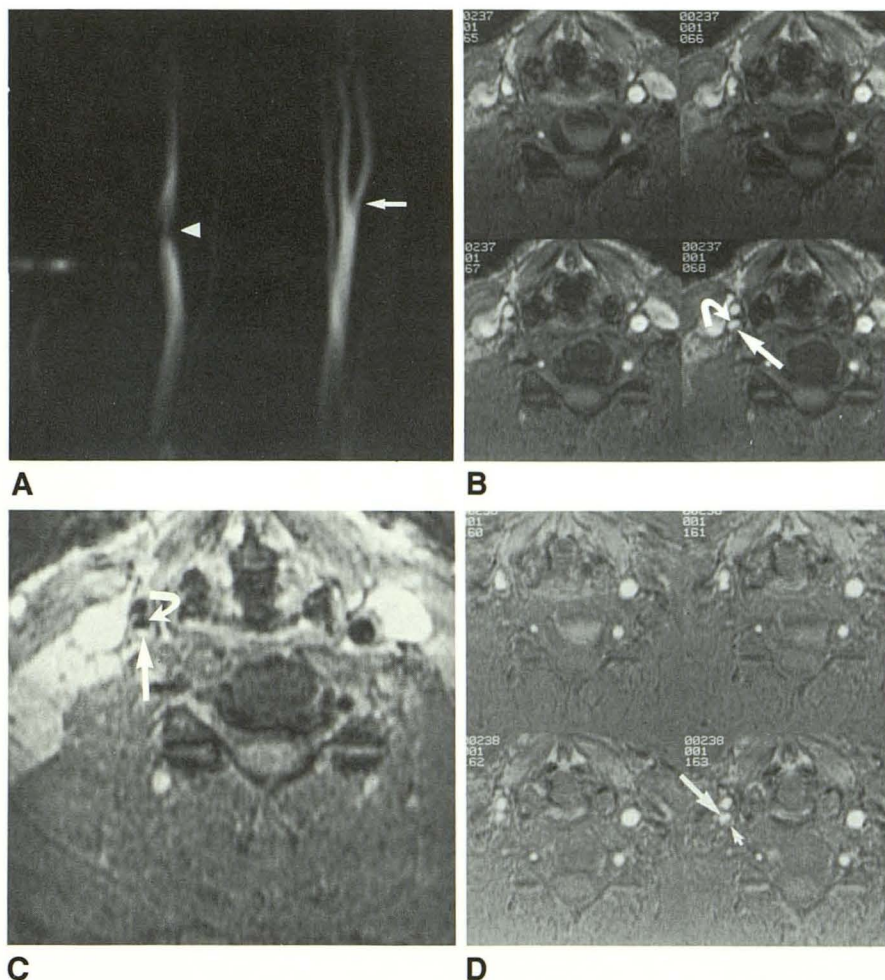

A

B

C

D

A

B

C

Fig. 6.—Case 5.

A, Left cervical internal carotid artery dissecting aneurysm just below skull base (*arrow*).

B, Phase-contrast-projection angiogram shows dissecting aneurysm just below skull base (*arrow*).

C, 3DFT nonsaturation with contiguous 1.25-mm axial images shows narrowed left internal carotid artery (*short straight arrow*), large dissecting aneurysm (*curved arrow*), and fine, low-signal wall separating the two (*long straight arrow*).
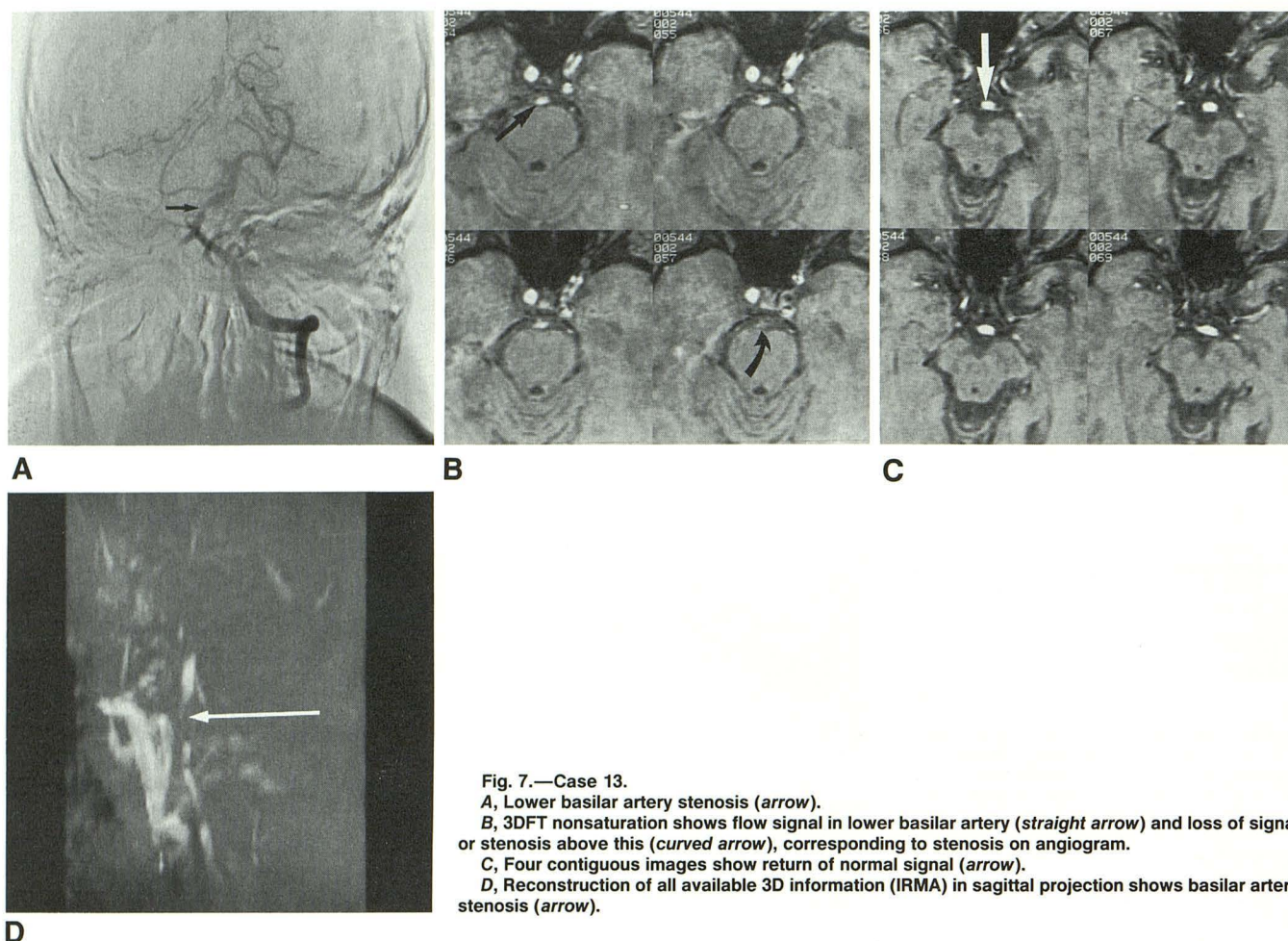
A

B

C

D

Fig. 7.—Case 13.
A, Lower basilar artery stenosis (arrow).
B, 3DFT nonsaturation shows flow signal in lower basilar artery (straight arrow) and loss of signal or stenosis above this (curved arrow), corresponding to stenosis on angiogram.
C, Four contiguous images show return of normal signal (arrow).
D, Reconstruction of all available 3D information (IRMA) in sagittal projection shows basilar artery stenosis (arrow).

three vectors on a pixel-by-pixel basis. This will increase the time of the study because three different flow images (x, y, and z) need to be obtained.

BINOP is a postprocessing function of image data and does not increase the amount of time that the patient must spend in the MR unit. BINOP addition or subtraction of data sets takes about 1 hr. The other postprocessing function, IRMA, is used to reproject data from 3DFT data sets, but this operation can take several hours to perform.

3DFT time-of-flight angiography has several advantages over 2DFT projection phase-contrast angiography; the most important is that signal loss due to complex flow and turbulence is decreased by the use of velocity-compensated gradients for all gradient functions. Phase-encoding artifacts due to pulsatile flow are also reduced. Time-of-flight procedures can be designed to exploit only longitudinal magnetization and thus be insensitive to flow-induced phase shifts in transverse magnetization. The greatest limitations on the time-of-flight technique are the inability to visualize vessels with very slow flow and the restriction of imaging to relatively small areas within the body. The latter is due to the short T1 of flowing blood. By analogy, the distance that the tagged flowing blood travels during its "flight" within the region of interest is a function of its velocity and the time (T1) it is able

to "fly." Therefore, it is essential to select an FOV and excitation slab that centers closely around the area of interest, typically the carotid artery bifurcation.

Our experience with the 2DFT projection phase-contrast technique for determining the presence or absence of flow within a vessel has been very encouraging, but it has marked limitations in determining the degree of stenosis within that vessel. In case 10 (Fig. 3), the MR angiogram demonstrated the return of flow within an internal carotid artery that was shown to be occluded on an angiogram obtained 2 months earlier. Although there was no follow-up angiogram to prove this, a Doppler sonographic study showed return of flow within this same artery. This occurred in a patient with a carotid artery dissection who was treated with heparin and Coumadin. Return of flow within an occluded artery has been described previously in cases of carotid artery dissection [11– 13].

A single-view phase-contrast angiogram can be obtained in only a few minutes, but we have found it very useful to obtain multiple view angles in order to correctly identify vessels and to localize the carotid artery bifurcation. After this, a series of 3DFT images is obtained in 20 min, and postprocessing can be performed after the patient has been removed from the magnet. Images can be viewed in a dynamic fashion

with the use of cine or spatial mode on a CRT. The technique is entirely noninvasive, relatively fast, and appears to have achieved a high degree of spatial resolution. Study of a large series is now underway that will compare this technique with standard angiography. New techniques for postprocessing of information and new pulse sequences for evaluation of the intracranial vasculature are being developed.

REFERENCES

1. Dumoulin CL, Cline HE, Souza SP, Wagle WA, Walker MF. Three dimensional time-of-flight magnetic resonance angiography using spin saturation. *Magn Reson Med* **1989**;11:35–46
2. Singer JR. Blood flow rates by nuclear magnetic resonance. *Science* **1959**;130:1652–1653
3. Wehrli FW, Shimakawa A, MacFall JR, Axel L, Perman W. MR imaging of venous and arterial flow by a selective saturation-recovery spin echo (SSRSE) method. *J Comput Assist Tomogr* **1985**;9:537–545
4. Wedeen VJ, Reto AM, Edelman RR, et al. Projective imaging of pulsatile flow with magnetic resonance. *Science* **1985**;230:946–948
5. Bradley WG, Waluch V. Blood flow: magnetic resonance imaging. *Radiology* **1985**;154:443–450
6. Masaryk TJ, Ross JS, Modic MT, et al. Magnetic resonance imaging of the carotid bifurcation: work in progress. *Radiology* **1988**;166:461–466
7. Dumoulin CL, Hart HH. Magnetic resonance angiography. *Radiology* **1986**;161:717–720
8. Wood GW, Dumoulin CL, Souza SP, Wagle WA, Hart HH, Eames FA. Magnetic resonance angiography of craniocervical vascular lesions. Presented at the annual meeting of the American Society of Neuroradiology, New York City, May **1987**
9. Cline HE, Dumoulin CL, Hart HR, Lorensen WE, Ludke S. 3D reconstruction of the brain from magnetic resonance images using a connectivity algorithm. *Magn Reson Imaging* **1987**;5:345–352
10. Wehrli FW, MacFall JR, Newton TH. Parameters determining the appearance of NMR images. In: Newton TH, Potts DG, eds. *Modern neuroradiology*, vol. 2. San Anselmo, CA: Clavadel, **1983**:87–89
11. Alpert JN, Gerson LP, Hall RJ, et al. Reversible angiopathy. *Stroke* **1982**;13:100–105
12. Mokri B, Piepgras DG, Houser OW. Traumatic dissections of the extracranial carotid artery. *J Neurosurg* **1988**;68:189–197
13. Houser OW, Mokri B, Sundt TM Jr, et al. Spontaneous cervical cephalic arterial dissection and its residuum: angiographic spectrum. *AJNR* **1984**;5:27–34